5. G. Auerbach *et al*., *EMBO J.* **16**, 7219 (1997).
6. D. Seeliger, B. L. de Groot, *Proteins* **68**, 595 (2007).
7. R. S. Rowland, R. Taylor, *J. Phys. Chem.* **100**, 7384 (1996).
8. L. Bonafé, B. Thöny, J. M. Penzien, B. Czarnecki, N. Blau, *Am. J. Hum. Genet.* **69**, 269 (2001).
9. T. Kenakin, *A Pharmacology Primer* (Elsevier, London, ed. 3, 2009), pp. 184–188.
10. J. Helweg-Larsen, T. Benfield, C. Atzori, R. F. Miller, *J. Antimicrob. Chemother.* **64**, 1282 (2009).
11. M. Harigai, R. Koike, N. Miyasaka, *N. Engl. J. Med.* **357**, 1874 (2007).
12. R. C. Stevens, S. C. Laizure, C. L. Williams, D. S. Stein, *Antimicrob. Agents Chemother.* **35**, 1884 (1991).
13. L. E. Walker *et al*., *J. Antimicrob. Chemother.* **66**, 1117 (2011).
14. K.-Y. Lee *et al*., *J. Antimicrob. Chemother.* **67**, 2749 (2012).
15. A. E. Cribb, B. L. Lee, L. A. Trepanier, S. P. Spielberg, *Adverse Drug React. Toxicol. Rev.* **15**, 9 (1996).
16. C. S. Keefer, *N. Engl. J. Med.* **226**, 266 (1942).
17. H. B. van Dyke, *Ann. N. Y. Acad. Sci.* **44**, 477 (1943).
18. T. Pullar, *Adverse Drug React. Toxicol. Rev.* **11**, 93 (1992).
19. E. K. Marshall, J. T. Litchfield, *J. Pharmacol. Exp. Ther.* **67**, 454 (1939).
20. J. F. Sadusk, J. W. Hirshfeld, A. Seymour, *Yale J. Biol. Med.* **13**, 351 (1941).
21. T. Sakai, T. Matsuishi, S. Yamada, H. Komori, H. Iwashita, *J. Neural Transm. Gen. Sect.* **102**, 159 (1995).
22. R. C. Woody, M. A. Brewster, *Dev. Med. Child Neurol.* **32**, 639 (1990).
23. J. L. Biedler, S. Roffler-Tarlov, M. Schachner, L. S. Freedman, *Cancer Res.* **38**, 3751 (1978).
24. M. Bräutigam, R. Dreesen, H. Herken, *J. Neurochem.* **42**, 390 (1984).
25. D. W. Macartney, R. W. Luxton, G. S. Smith, W. A. Ramsay, J. Goldman, *Lancet* **239**, 639 (1942).
26. O. Sugita, Y. Sawada, Y. Sugiyama, T. Iga, M. Hanano, *J. Pharmacokinet. Biopharm.* **10**, 297 (1982).
27. O. Lacombe *et al*., *Mol. Pharm.* **8**, 651 (2011).
28. J. Drews, *Science* **287**, 1960 (2000).
29. Y. L. Hong *et al*., *J. Eukaryot. Microbiol.* **43**, 40S (1996).

Acknowledgments: The authors thank G. Turcatti, M. Chambon, M. Busquets, and M. Rengifo González for technical assistance; the Swiss Light Source for support during x-ray data collection; and G. Lukinavicius, O. Sallin, P. Hauser, and C. Woolf for helpful discussions. This work was supported by EPFL, the Swiss National Science Foundation, and the NCCR Chemical Biology. Coordinates and structure factors for the crystal structures have been deposited in the Protein Data Bank (PDB), and the PDB accession codes are listed in table S8.

Supplementary Materials

www.sciencemag.org/cgi/content/full/340/6135/987/DC1
Materials and Methods
Figs. S1 to S3
Tables S1 to S8
References (*30*–*82*)

19 November 2012; accepted 8 April 2013
10.1126/science.1232972

Defining Single Molecular Forces Required to Activate Integrin and Notch Signaling

Xuefeng Wang[1] and Taekjip Ha[1,2]*

Cell-cell and cell-matrix mechanical interactions through membrane receptors direct a wide range of cellular functions and orchestrate the development of multicellular organisms. To define the single molecular forces required to activate signaling through a ligand-receptor bond, we developed the tension gauge tether (TGT) approach in which the ligand is immobilized to a surface through a rupturable tether before receptor engagement. TGT serves as an autonomous gauge to restrict the receptor-ligand tension. Using a range of tethers with tunable tension tolerances, we show that cells apply a universal peak tension of about 40 piconewtons (pN) to single integrin-ligand bonds during initial adhesion. We find that less than 12 pN is required to activate Notch receptors. TGT can also provide a defined molecular mechanical cue to regulate cellular functions.

Cells sense and respond to the mechanical properties of the surrounding extracellular matrix (ECM) and neighboring cells. Reciprocally, cells also apply force on the ECM and transmit mechanical signals to neighboring cells. These mechanical interactions activate intracellular signaling pathways and regulate such diverse processes as cell adhesion, polarization, migration, proliferation, and differentiation (*1*, *2*). As a result, by tuning bulk mechanical properties like stiffness, texture, and geometry of the substrate, researchers have gained insight into processes such as stem cell differentiation (*3*) and tumor metastasis (*4*). Single-molecule force spectroscopy has been used to study various mechanosensitive membrane receptors, including integrin, cadherin, and Notch (*5*–*8*). However, these approaches cannot reveal the single-molecule forces required for physiological functions because they either measure collective forces exerted through many molecules or probe molecular unbinding or unfolding forces only. More recently, fluorescence resonance energy transfer–based force sensors were developed and inserted to target sites to monitor cellular forces (*9*, *10*), but great efforts must be taken to prepare the sensors and to track and interpret the fluorescence signal. Here, we describe a platform termed tension gauge tether (TGT) that allows us to determine the single-molecule forces required for mechanical signaling in cells.

In TGT, a ligand is covalently conjugated to a tether that ruptures at a critical force, which we term "tension tolerance" or T_{tol}, and is immobilized on a solid surface through the tether (Fig. 1). Cells are plated on the surface, and membrane receptors engage with and apply tension to the ligands. If signal activation through the receptor requires a molecular tension larger than T_{tol}, the tether will rupture, abolishing signal activation. In contrast, if the required tension is smaller than T_{tol}, the tether will endure, activating the receptor-mediated signaling. By engineering a series of tethers with different T_{tol} values, the tension required for signal activation can be determined by observing receptor-regulated cell activities, which are usually much easier to detect than single-molecule events. Because each ligand is equipped with an individual tension gauge, the measurement is independent of the receptor or ligand density.

DNA is a good candidate for use as rupturable tether in TGT because force application geometry (fig. S1) strongly affects its rupture force, with an unzipping force rupturing the DNA at a much lower force than a shearing force (*11*, *12*). Albrecht *et al*. have exploited this feature to estimate the rupture force of an antigen-antibody bond relative to the rupture forces of double-stranded DNA (dsDNA) in unzipping or shear geometry (*13*). The estimated rupture force of a 21–base pair (bp) DNA is about 12 pN in the unzipping geometry and is about 56 pN in the shear geometry (*14*). Intermediate rupture forces can be obtained by applying forces through an internal position on the DNA duplex, and the theoretical T_{tol} values of the resulting tethers can be estimated (Fig. 1D and fig. S2). T_{tol} represents the force required to rupture the tether in less than 2 s when the force is applied at a constant level (*12*) [see supplementary text (*14*)].

Integrins are membrane receptors that mediate cell adhesion and sense and transduce mechanical information from the ECM into cells. Bulk traction forces applied through a collection of integrin-ligand bonds have been extensively examined (*15*–*18*). Here, we apply the TGT platform to probe the tension on a single integrin-ECM ligand bond required for cell adhesion (specifically, integrin $\alpha_V\beta_3$ and its ligand, cyclic RGDfK peptide). To reduce nonspecific adhesion, ligands with the DNA tether are immobilized through an Avidin-biotin linker on a glass surface passivated with polyethylene glycol (PEG). The Avidin-biotin unbinding force, ~160 pN (*19*), is much larger than the tether rupture forces used here (≤56 pN).

We conjugated RGDfK to nine different DNA tethers with estimated T_{tol} values of 12, 16, 23, 33, 43, 50, 54, 55, and 56 pN (fig. S2). These DNA tethers have various force application geometries but share the same length, sequence, and thermal stability. A TGT array was created by

[1]Department of Physics, Center for the Physics of Living Cells and Institute for Genomic Biology University of Illinois at Urbana-Champaign, Urbana, IL 61801, USA. [2]Howard Hughes Medical Institute, Urbana, IL 61801, USA.

*Corresponding author. E-mail: tjha@illinois.edu

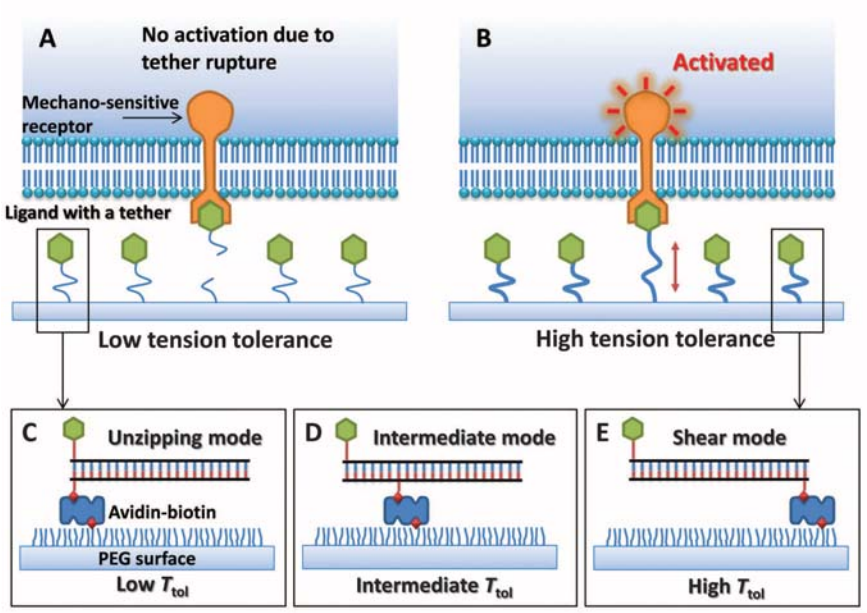

Fig. 1. Principle of TGT. A ligand for a membrane receptor is immobilized on the surface through a tether that ruptures if the tension applied by the cell through the receptor is larger than its T_{tol}. Signaling through the receptor is not activated if the tension required for activation exceeds T_{tol} and ruptures the tether (**A**) and is activated if T_{tol} is larger than the required tension (**B**). (**C** to **E**) DNA duplex helix as a tether with tunable T_{tol} values.

depositing the nine constructs as 2-mm-diameter spots at a surface ligand density of 600 molecules/μm^2 (Fig. 2A) (see calibration in fig. S3). CHO-K1 cells were incubated on this surface for 30 min at a density of 1×10^6 cells/mL. The surface was gently rinsed, and unbound cells were removed through media exchange. Phase-contrast images were taken to measure the cell density.

We observed little cell adhesion for DNA tethers with $T_{tol} \leq 33$ pN and significant adhesion for $T_{tol} \geq 43$ pN with the cell counts increasing slightly with increasing T_{tol} (Fig. 2, B and C), suggesting that the peak tension CHO-K1 cells generate on a single RGDfK-integrin $\alpha_V\beta_3$ bond during adhesion lies mostly in the range of 33 to ~43 pN. To examine the effect of ligand density, we created the same TGT surface with lower ligand densities and arrived at the same tension threshold for cell adhesion (fig. S4). Other cell lines were also tested: MDA-MB-231, HeLa, HEK 293, and NIH/3T3 cells. Remarkably, all of the measured molecular tension thresholds fall within the same range, with the largest increase in cell counts occurring between a T_{tol} of 33 and 43 pN (Fig. 2D and fig. S5). In contrast, bulk traction forces normally vary among different

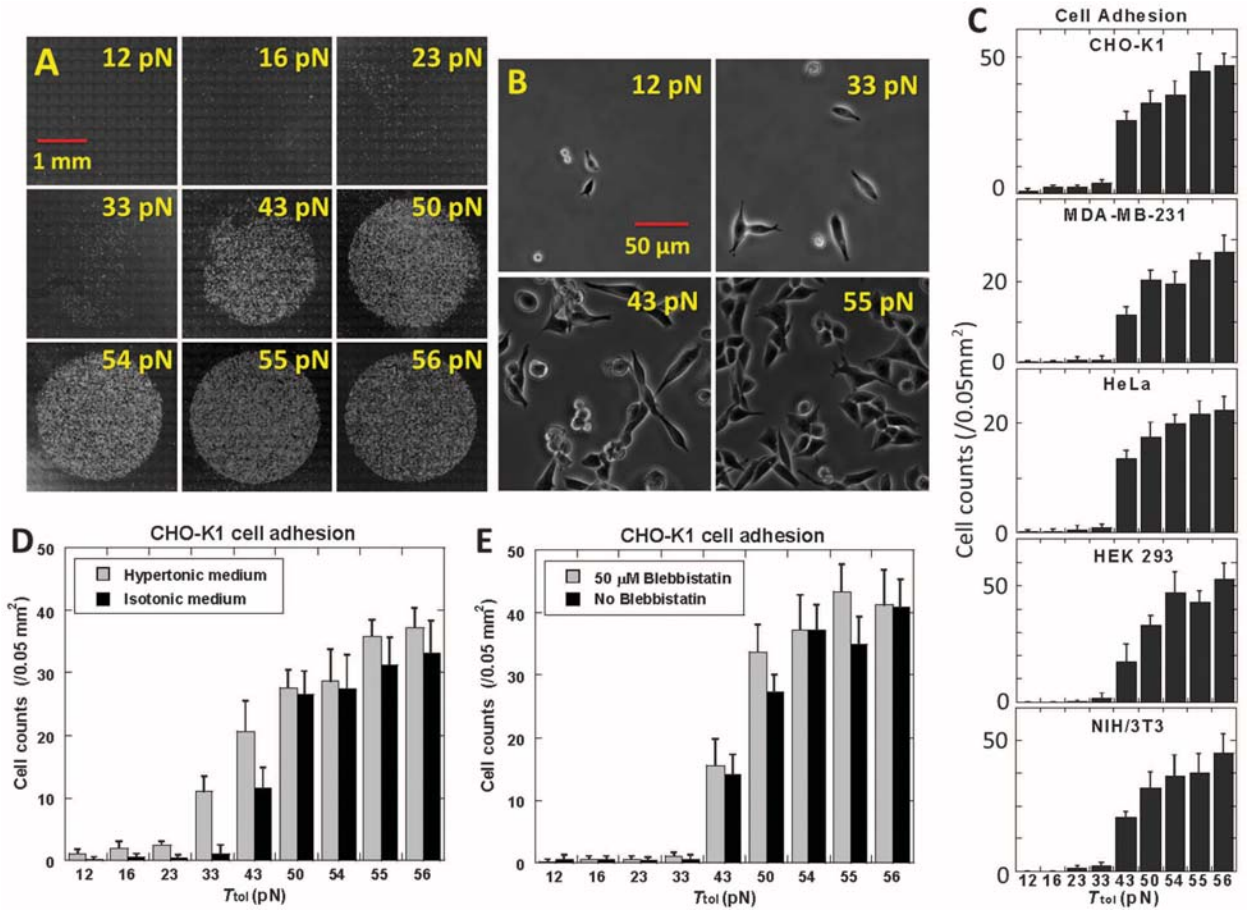

Fig. 2. Cell adhesion on TGT with RGDfK. (**A**) Phase-contrast images of adherent CHO-K1 cells (white dots) on circular regions coated with nine TGT constructs of RGDfK-conjugated dsDNA with the indicated T_{tol} values. (**B**) Zoomed-in phase-contrast images of CHO-K1 cells on four of the regions. (**C**) Cell density (counts per 0.05 mm^2) as a function of T_{tol} for five different cell lines as indicated. (**D**) Cell density versus T_{tol} for CHO-K1 cells in hypertonic versus isotonic medium. (**E**) Cell density versus T_{tol} for CHO-K1 cells with and without 50 μM Blebbistatin. Error bars, mean ± SD (n = 8 cell counting regions).

cell lines (*20*–*22*). Our observation suggests that there exists a common tension threshold value for the molecular tension generated by cells on an active integrin $\alpha_V\beta_3$ during adhesion. The same tension threshold was observed for cell seeding times as short as 5 min (figs. S6 and S7).

Using constructs that cannot be ruptured but have similar ligand accessibility as the TGTs and additional constructs with similar ligand accessibility but with different force application geometries, we could ensure that the close proximity of the ligand and biotin in the low T_{tol} constructs does not reduce ligand accessibility and cause poor cell adhesion (fig. S8). We also confirmed that the tether indeed ruptures in low T_{tol} constructs by labeling RGDfK-conjugated DNA strand with Cy3 fluorophore and observing the loss of fluorescence under the cell plating sites (figs. S9 and S10).

Because integrins are membrane proteins that are anchored to the cytoskeleton, the cell membrane and the cytoskeleton are two potential determinants of the tension threshold. We used a hypertonic medium to reduce the membrane tension and the myosin II inhibitor blebbistatin to reduce the cytoskeleton tension. The tension threshold shifted to 23 to ~33 pN for cells in the hypertonic medium (150 mM sucrose), as compared with 33 to ~43 pN in an isotonic medium (Fig. 2E and fig. S11). In contrast, the tension threshold remained unchanged with 0 to 100 μM blebbistatin (Fig. 2E and figs. S12 and S13). Cell morphology changes confirmed the efficacy of the blebbistatin treatment (fig. S14). The data suggests that molecular tension on integrins during the initial stages of cell adhesion is primarily regulated by the membrane tension, reminiscent of a recent study that found the membrane tension to play a dominant role in restricting actin assembly and Rac activation in the leading-edge protrusion of migrating cells (*23*).

We next examined the formation of focal adhesions (FAs), which can occur following initial cell adhesion and spreading. FAs consist of clusters of integrins and other adaptor proteins such as vinculin, talin, and paxillin, and their formation requires a mechanical stimulus (*24*, *25*). We asked whether the measured ~40 pN tension threshold reflects initial cell adhesion or FA formation. On a regular petri dish surface, CHO-K1 cells formed FAs and well-organized stress fibers, as detected through vinculin immunostaining and F-actin staining by phalloidin–tetramethyl rhodamine isothiocyanate, respectively (fig. S15). We seeded CHO-K1 cells for 30 min, 1 hour, and 2 hours on two TGT surfaces, one with the highest T_{tol} = 56 pN and the other with T_{tol} = 43 pN, which is just above the tension threshold for adhesion. At the 30-min seeding time, cells adhered and spread on both surfaces, but vinculin remained diffusive and stress fibers did not form on either surface (fig. S16), confirming that the initial stages of cell adhesion and FA formation are two separate stages. Together with the observation that the threshold tension for adhesion takes effect at an early time point (5 min) of initial cell spreading, which typically lasts 15 min and is independent of talin (*26*), we conclude that ~40 pN tension, which is required for initial cell adhesion, acts before FA formation. We speculate that integrins may work alone without clustering in the initial stages of cell adhesion, resulting in our observed common tension threshold for different cell lines. At the 1-hour seeding time, FAs and stress fibers started to form on the 56 pN surface but not on the 43 pN surface (fig. S16). After 2 hours, FAs and stress fibers were well formed on the 56 pN surface but still not on the 43 pN surface (Fig. 3). Thus FA formation requires a molecular tension larger than that required for initial cell adhesion.

Next, we examined the molecular tension required for Notch receptor activation using a fluorescence reporter, H2B-YFP (yellow fluorescent protein). The Notch signaling pathway is responsible for intercellular communication, cell differentiation, and cell fate determination. The Notch receptor, a transmembrane protein, is activated by binding to its ligands on the neighboring cell's membrane (*27*). Several studies have implicated mechanical forces in Notch activation. For example, a force applied to a Notch-ligand bond may expose a cleavage site of Notch to initiate activation (*28*–*30*).

To determine the force required, we conjugated a Notch ligand DDL1 (delta-like protein 1) to a DNA strand and bovine serum albumin (BSA) to the complementary strand. DLL1-DNA (25 nM) was annealed to BSA-DNA immobilized on a glass coverslip treated with fibronectin. After blocking the surface with free BSA, we seeded CHO-K1 cells stably expressing human NOTCH1 with its intracellular domain replaced by the activator $Gal4^{esn}$. This cell line was also transfected with $Gal4^{esn}$-controlled H2B-YFP. After notch activation, H2B-YFP fluorescence was detected in the nucleus, reaching an optimal level after 2 days (*31*). We tested 24-bp DNA tethers, one in unzipping and the other in shear geometry with an estimated T_{tol} of 12 and 58 pN, respectively. Cells on both surfaces expressed H2B-YFP, indicating Notch activation (Fig. 4, A and B). As a control, a surface with TGT in the unzipping configuration was further treated with DNase I, which cleaves the DNA tether. As another control, DLL1-DNA conjugate was incubated with a surface coated with free BSA only (i.e., no complementary strand on the surface). On both surfaces, the YFP fluorescence level was dramatically lower (Fig. 4, C and D), ruling out the possibility that Notch is activated by nonspecifically adsorbed DLL1. Other tethers with T_{tol} = 45, 50, and 53 pN all resulted in Notch activation (fig. S17). We conclude that Notch activation requires either no tension or a tension below 12 pN.

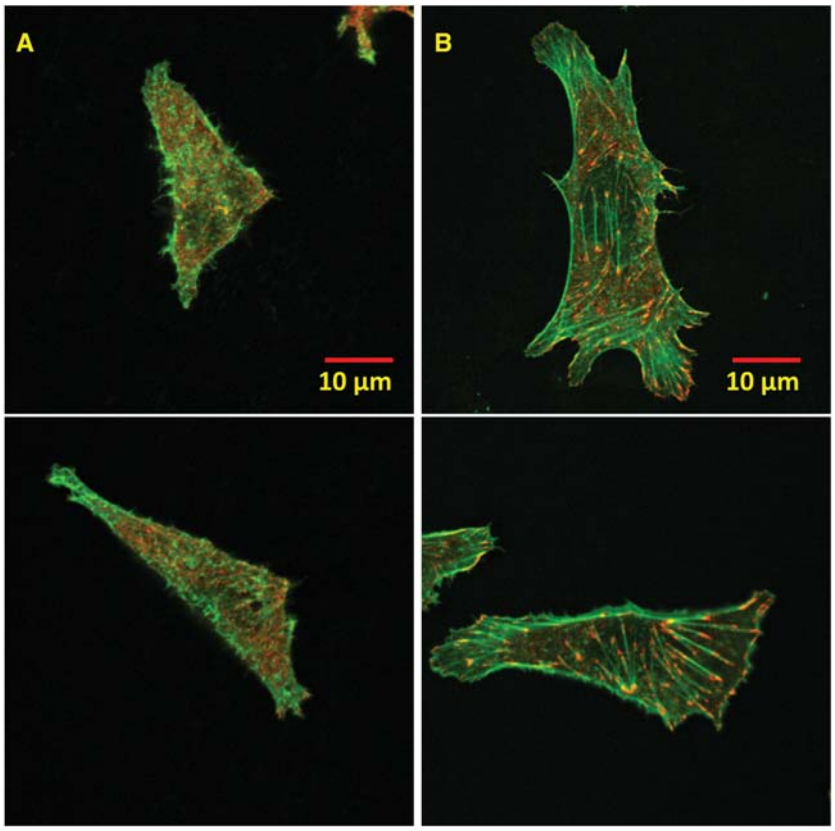

Fig. 3. Confocal fluorescent images of CHO-K1 cells. (**A**) A 43-pN TGT surface. (**B**) A 56-pN TGT surface. Actin in green and vinculin in red. Images were obtained after 2-hour cell plating. Bright green lines in (B) are stress fibers that terminate in focal adhesion complexes marked in red.

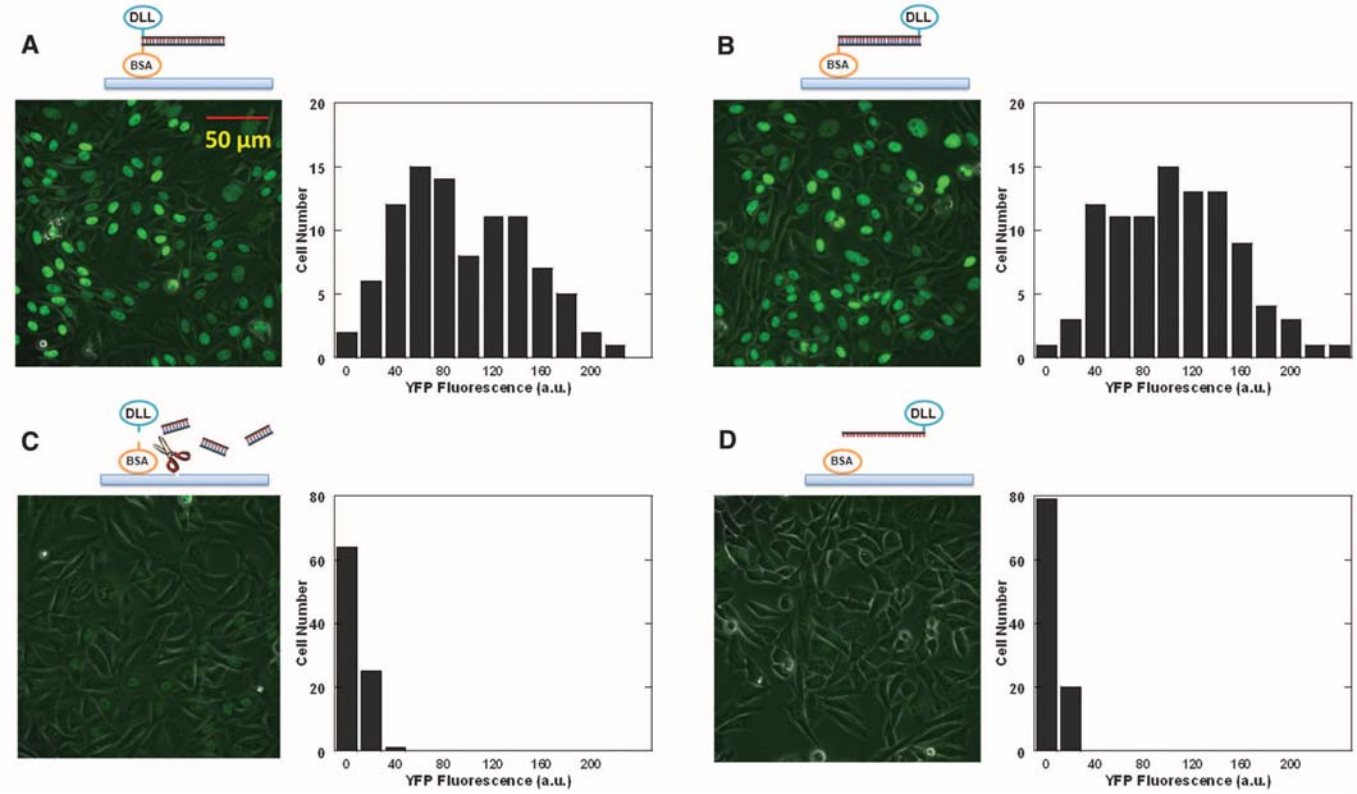

Fig. 4. H2B-YFP expression in the nucleus as a reporter of Notch activation. (**A** to **D**) YFP fluorescence images of CHO-K1 cells show nuclear fluorescence of H2B-YFP when Notch is activated. Histograms of fluorescence intensities of single cells are also shown. a.u., arbitrary unit. (A) T_{tol} = 12 pN. (B) T_{tol} = 58 pN. (C) 12-pN TGT with DNase I digestion. (D) A control with unconjugated BSA. Here, we used BSA for TGT immobilization and surface passivation because PEG surface did not survive the 2-day period required for our Notch reporter system.

We used TGT mainly as a measurement tool here, but it can also provide a defined single-molecule mechanical cue to the cells, as we demonstrated by showing that T_{tol} values control the formation of stress fibers and FAs. It is well known that mechanical cues stemming from substrate stiffness or micropatterning can affect cancer cell or stem cell behaviors (*1*, *32*). Tunable mechanical properties that have been examined were bulk features such as compliance, texture, and geometry. However, the sensors of mechanical cues are normally composed of single molecules, and questions remain about how a receptor as a single molecule can sense bulk properties such as stiffness. We suggest that the TGT platform provides a viable means to address these questions.

References and Notes

1. D. E. Discher, P. Janmey, Y. L. Wang, *Science* **310**, 1139 (2005).
2. B. D. Hoffman, C. Grashoff, M. A. Schwartz, *Nature* **475**, 316 (2011).
3. A. J. Engler, S. Sen, H. L. Sweeney, D. E. Discher, *Cell* **126**, 677 (2006).
4. K. R. Levental *et al.*, *Cell* **139**, 891 (2009).
5. R. Merkel, P. Nassoy, A. Leung, K. Ritchie, E. Evans, *Nature* **397**, 50 (1999).
6. N. Wang, J. P. Butler, D. E. Ingber, *Science* **260**, 1124 (1993).
7. Y. X. Wang *et al.*, *Nature* **434**, 1040 (2005).
8. B. Shergill, L. Meloty-Kapella, A. A. Musse, G. Weinmaster, E. Botvinick, *Dev. Cell* **22**, 1313 (2012).
9. C. Grashoff *et al.*, *Nature* **466**, 263 (2010).
10. D. R. Stabley, C. Jurchenko, S. S. Marshall, K. S. Salaita, *Nat. Methods* **9**, 64 (2012).
11. B. Essevaz-Roulet, U. Bockelmann, F. Heslot, *Proc. Natl. Acad. Sci. U.S.A.* **94**, 11935 (1997).
12. K. Hatch, C. Danilowicz, V. Coljee, M. Prentiss, *Phys. Rev. E Stat. Nonlin. Soft Matter Phys.* **78**, 011920 (2008).
13. C. Albrecht *et al.*, *Science* **301**, 367 (2003).
14. Materials and methods and additional information are available as supplementary materials on *Science* Online.
15. A. K. Harris, D. Stopak, P. Wild, *Nature* **290**, 249 (1981).
16. A. K. Harris, P. Wild, D. Stopak, *Science* **208**, 177 (1980).
17. N. Q. Balaban *et al.*, *Nat. Cell Biol.* **3**, 466 (2001).
18. J. L. Tan *et al.*, *Proc. Natl. Acad. Sci. U.S.A.* **100**, 1484 (2003).
19. V. T. Moy, E. L. Florin, H. E. Gaub, *Science* **266**, 257 (1994).
20. Z. Li *et al.*, *Nano Lett.* **9**, 3575 (2009).
21. S. Munevar, Y. L. Wang, M. Dembo, *Biophys. J.* **80**, 1744 (2001).
22. J. X. Chen, H. X. Li, N. SundarRaj, J. H. C. Wang, *Cell Motil. Cytoskeleton* **64**, 248 (2007).
23. A. R. Houk *et al.*, *Cell* **148**, 175 (2012).
24. D. Riveline *et al.*, *J. Cell Biol.* **153**, 1175 (2001).
25. P. W. Oakes, Y. Beckham, J. Stricker, M. L. Gardel, *J. Cell Biol.* **196**, 363 (2012).
26. X. Zhang *et al.*, *Nat. Cell Biol.* **10**, 1062 (2008).
27. S. Artavanis-Tsakonas, M. D. Rand, R. J. Lake, *Science* **284**, 770 (1999).
28. W. R. Gordon *et al.*, *Nat. Struct. Mol. Biol.* **14**, 295 (2007).
29. B. Varnum-Finney *et al.*, *J. Cell Sci.* **113**, 4313 (2000).
30. A. L. Parks, K. M. Klueg, J. R. Stout, M. A. Muskavitch, *Development* **127**, 1373 (2000).
31. D. Sprinzak *et al.*, *Nature* **465**, 86 (2010).
32. K. Salaita *et al.*, *Science* **327**, 1380 (2010).

Acknowledgments: We thank I. D. Bernstein for the generous gift of DLL1. We also appreciate the genetically modified CHO-K1 cell line for Notch study provided by M. B. Elowitz. We thank Q. Xu, N. Wang, and Y. Wang for carefully reading the manuscript. Funding was provided by the National Science Foundation through the Physics Frontiers Center Program (0822613). T.H. is an investigator with the Howard Hughes Medical Institute.

Supplementary Materials

www.sciencemag.org/cgi/content/full/340/6135/991/DC1
Materials and Methods
Supplementary Text
Figs. S1 to S17
References (*33*–*37*)

3 October 2012; accepted 19 March 2013
10.1126/science.1231041